Solvable Dynamics of Coupled High-Dimensional Generalized Limit-Cycle Oscillators

Wei Zou [1,*] Sujuan He,[1] D. V. Senthilkumar,[2] and Jürgen Kurths [3,4,5]

[1]*School of Mathematical Sciences, South China Normal University, Guangzhou 510631, China*
[2]*School of Physics, Indian Institute of Science Education and Research, Thiruvananthapuram 695551, Kerala, India*
[3]*Potsdam Institute for Climate Impact Research, Telegraphenberg, Potsdam D-14415, Germany*
[4]*Institute of Physics, Humboldt University Berlin, Berlin D-12489, Germany*
[5]*Research Institute of Intelligent Complex Systems, Fudan University, Shanghai 200433, China*

We introduce a new model consisting of globally coupled high-dimensional generalized limit-cycle oscillators, which explicitly incorporates the role of amplitude dynamics of individual units in the collective dynamics. In the limit of weak coupling, our model reduces to the D-dimensional Kuramoto phase model, akin to a similar classic construction of the well-known Kuramoto phase model from weakly coupled two-dimensional limit-cycle oscillators. For the practically important case of $D = 3$, the incoherence of the model is rigorously proved to be stable for negative coupling ($K < 0$) but unstable for positive coupling ($K > 0$); the locked states are shown to exist if $K > 0$; in particular, the onset of amplitude death is theoretically predicted. For $D \geq 2$, the discrete and continuous spectra for both locked states and amplitude death are governed by two general formulas. Our proposed D-dimensional model is physically more reasonable, because it is no longer constrained by fixed amplitude dynamics, which puts the recent studies of the D-dimensional Kuramoto phase model on a stronger footing by providing a more general framework for D-dimensional limit-cycle oscillators.

Self-organization of collective behavior from interacting units is ubiquitous in nature [1–4], which can be qualitatively and quantitatively explored by employing models of coupled nonlinear oscillators [5–7]. Among them, the celebrated Kuramoto model [8] has served as a paradigm for the study of synchronization in wide disciplines ranging from physics to biology to engineering [9–11]. For a better understanding of the mechanisms of synchronization, Ritort [12] introduced a solvable model of interacting random tops incorporating the orientational degree of freedom, which in fact extends the Kuramoto model with noise to three dimensions [13]. Later on, the D-dimensional Kuramoto model has been further proposed [14–16], where all the individual oscillators (agents) are interpreted as D-dimensional unit vectors, rotating on the surface of the D-dimensional sphere. Quite recently, Chandra, Girvan, and Ott [17] systematically examined the dynamics of the D-dimensional generalized Kuramoto model with heterogeneous natural rotations; in particular, they unveiled that the nature of phase transition for the generalized Kuramoto model with an odd number of dimensions is remarkably different from that in even dimensions. Since then, there has been a burst of appealing works devoted to the study of the D-dimensional generalized Kuramoto model and its variants [18–25].

However, the amplitude dynamics of individual units has not been taken into account in the above studies. This strongly limits the applicability of the model, as the amplitude degree of freedom generally plays a key role in determining the collective dynamics of strongly coupled systems, with

examples including a flock of birds, a school of fish, a swarm of flying drones or insects [26–29], etc. Phase-amplitude models are deemed to capture common neuroimaging metrics more accurately and are important to quantify anesthetized brain states [30]. A full representation of the phase and amplitude coordinates is of particular relevance for understanding the bifurcations of high-dimensional nonlinear systems beyond the weak coupling limit [31].

To resolve this limitation, in this Letter, we propose a new model of globally coupled D-dimensional generalized limit-cycle oscillators, which explicitly incorporates both the phase and amplitude dynamics of individual units. Our model includes the D-dimensional Kuramoto phase model as a special case in the weak coupling limit. Of particular interest, we show that our model for the practically important case of $D = 3$ is solvable in the thermodynamic limit, which provides a new paradigmatic example of analytically tractable models. The high-dimensional model proposed in this Letter is expected to better capture emergent dynamics in diverse physical and biological systems comprised of interacting units with natural magnetic moments [32–34], such as strongly coupled magnetic particles [35–37] and microfluidic mixtures of active spinners [38,39].

The model consists of a system of N globally coupled D-dimensional vectors $\vec{r}_i \in \mathbb{R}^D$ described by

$$\frac{d\vec{r}_i}{dt} = (1 - |\vec{r}_i|^2)\vec{r}_i + \mathbf{W}_i\vec{r}_i + \frac{K}{N}\sum_{j=1}^{N}(\vec{r}_j - \vec{r}_i), \quad (1)$$

with $i = 1, 2, \ldots, N$, where K is the coupling strength, and $\mathbf{W}_i$ is a real $D \times D$ antisymmetric (skew-symmetric) matrix with $D(D-1)/2$ independent components, which can be physically interpreted as the natural rotation of the ith agent [40]. Each $\mathbf{W}_i$ is coded by the vector $\vec{\omega}_i = (\omega_{1i}, \omega_{2i}, \ldots, \omega_{[D(D-1)/2]i})^T$ drawn from a normalized distribution $G(\vec{\omega})$. In the limit of $K \to 0$, Eq. (1) degenerates to the D-dimensional Kuramoto model [41]. For $D = 2$, Eq. (1) reduces to the model addressed in Refs. [42–46], where the single uncoupled unit (coined as the Stuart-Landau oscillator) represents a canonical form near a supercritical Hopf bifurcation [1]. For $K \to 0$, the first-order phase reduction to Eq. (1) with $D = 2$ results in the classic Kuramoto model [8]; the second-order phase-reduction approach leads to the *enlarged* Kuramoto model [47,48].

Collective behavior in the model of Eq. (1) can be conveniently described by an order parameter $\vec{p} = (1/N) \sum_{i=1}^{N} \vec{r}_i$, where $p = |\vec{p}|$ measures the degree of collective synchronization. Depending on K and the spread of $\vec{\omega}_i$, the model exhibits three types of steady behaviors: *incoherence*, *amplitude death*, and *locking*, in which the system evolves to statistical steady states, characterized by a stationary distribution of oscillators in the phase space and a constant $\vec{p}$.

Figure 1 shows numerical observations of p vs K for the system in Eq. (1) with $D = 2–7$ and $N = 5000$. The $D(D-1)/2$ upper-triangular elements of $\mathbf{W}_i$ are chosen randomly according to a normal distribution with zero mean and the standard deviation Δ—i.e., $\omega_{ji} \sim Norm(0, \Delta^2)$ for $j = 1, 2, \ldots, D(D-1)/2$—while the corresponding lower-triangular elements are set to cause $\mathbf{W}_i$ to be an antisymmetric matrix. With the above choices of $\mathbf{W}_i$'s, $\vec{p}$ always asymptotically reaches an equilibrium.
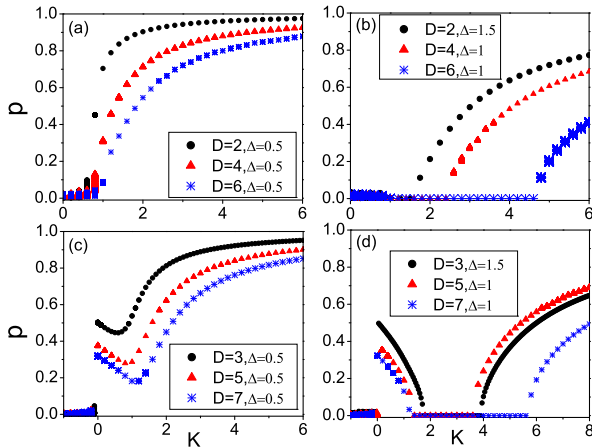

FIG. 1. The magnitude p of $\vec{p}$ vs K for the system in Eq. (1) with $N = 5000$ for $D = 2–7$. Each element of $\vec{\omega}_i = (\omega_{1i}, \omega_{2i}, \ldots, \omega_{[D(D-1)/2]i})^T$ is sampled randomly according to $Norm(0, \Delta^2)$. A small value of $\Delta = 0.5$ is used in the left column, while comparatively large values of Δ are employed in the right column.

We find that for all odd D, the transition from incoherence to coherence occurs discontinuously as K increases through zero (i.e., $K_c = 0$). In contrast, in the even-D case, the phase transition takes place continuously at $K_c > 0$. A similar difference in the nature of the phase transition between odd and even dimensions has been previously established in the D-dimensional Kuramoto model by Chandra *et al.* [17]. However, our high-dimensional model in Eq. (1) is no longer constrained by fixed amplitude dynamics, which may render the emergence of richer dynamics, such as amplitude death, as shown in the right column of Fig. 1 for large values of Δ. To predict the onset of emergent dynamics observed in Figs. 1(a)–1(d), we now conduct a theoretical analysis of the model [Eq. (1)] for $D \geq 3$.

i) Stability of incoherence. For $D = 3$, the incoherent state refers to the fact that each oscillator rotates rigidly around the vector $\hat{\omega}_i$ at its natural rotation rate ω_i on the sphere with a radius of $\sqrt{1-K}$ ($K < 1$), and meanwhile $\vec{p} = \vec{0}$ (i.e., $p = 0$) holds at all times. Strictly speaking, the incoherent solution exists only when $N \to \infty$, for which $\vec{p}$ becomes

$$\vec{p} = \int_{\mathbb{R}^3} \int_{\mathbb{R}^3} \vec{r} F(\vec{r}, \vec{\omega}, t) G(\vec{\omega}) d\vec{\omega} d\vec{r}, \quad (2)$$

where $F(\vec{r}, \vec{\omega}, t)$ represents a time-dependent joint density of $\vec{r}$ and $\vec{\omega}$, satisfying the continuity equation

$$\frac{\partial F}{\partial t} + \frac{\partial (F\dot{r})}{\partial r} + \frac{1}{\sin\theta} \frac{\partial (F \sin\theta \dot{\theta})}{\partial \theta} + \frac{\partial (F\dot{\phi})}{\partial \phi} = 0, \quad (3)$$

where $\dot{r}$, $\dot{\theta}$, and $\dot{\phi}$ can be calculated directly from Eq. (1) via introducing the spherical coordinates $\vec{r} = r\hat{r}$, with $\hat{r} = (\sin\theta\cos\phi, \sin\theta\sin\phi, \cos\theta)^T$. For the incoherence, the oscillators are uniformly distributed on the sphere with the radius $\sqrt{1-K}$ for each $\vec{\omega}$, and then the corresponding density is $F_0 = [\delta(r-a)/4\pi]$ with $a^2 = 1 - K$.

To analyze the linear stability of incoherence, we introduce a small perturbation to the incoherent solution as $F = F_0 + \varepsilon e^{st} \xi(r, \theta, \phi, \vec{\omega})$ ($0 < \varepsilon \ll 1$) [49]. Then the perturbed order parameter is

$$\vec{p} = \varepsilon e^{st} \int_{\mathbb{R}^3} \int_{\mathbb{R}^3} \vec{r} \xi G(\vec{\omega}) d\vec{\omega} d\vec{r} \triangleq \varepsilon e^{st} \langle \vec{\xi} \rangle. \quad (4)$$

Inserting the perturbed density into Eq. (3), we derive that

$$s\xi + \frac{\partial[(1-K-r^2)r\xi]}{\partial r} + \omega_\phi \frac{\partial \xi}{\partial \theta} - \frac{\omega_\theta}{\sin\theta} \frac{\partial \xi}{\partial \phi}$$
$$= \frac{K\delta(r-a)}{2\pi a} \langle \vec{\xi} \rangle \cdot \hat{r} - \frac{K\delta'(r-a)}{4\pi} \langle \vec{\xi} \rangle \cdot \hat{r}, \quad (5)$$

where $\omega_\theta = \vec{\omega} \cdot \hat{\theta}$, with $\hat{\theta} = (\cos\theta\cos\phi, \cos\theta\sin\phi, -\sin\theta)^T$, and $\omega_\phi = \vec{\omega} \cdot \hat{\phi}$, with $\hat{\phi} = (-\sin\phi, \cos\phi, 0)^T$, and

$\delta'(r-a) = d\delta(r-a)/dr$. The solution of ξ for Eq. (5) has the following form:

$$\xi = \frac{K\delta(r-a)}{2\pi a}\vec{A}\cdot\hat{r} - \frac{K\delta'(r-a)}{4\pi}\vec{B}\cdot\hat{r}, \qquad (6)$$

with $\vec{A} = (s\mathbf{I}-\mathbf{W})^{-1}\langle\vec{\xi}\rangle$ and $\vec{B} = [(s+2a^2)\mathbf{I}-\mathbf{W}]^{-1}\langle\vec{\xi}\rangle$. Substituting ξ from Eq. (6) into Eq. (4), the dispersion relation for s is obtained as [41]

$$\det\left(\mathbf{I} - \frac{2K}{3}\mathbf{J}(s) - \frac{K}{3}\mathbf{J}(s+2a^2)\right) = 0, \qquad (7)$$

where $\mathbf{J}(s) = \int_{\mathbb{R}^3}(s\mathbf{I}-\mathbf{W})^{-1}G(\vec{\omega})d\vec{\omega}$. If Eq. (7) has one root with a positive real part, the incoherent state is unstable.

Assuming that the rotation directions of individual oscillators are isotropically distributed on the unit sphere, and independent of the distribution of the rotation magnitudes $g(\omega)$, one can write $G(\vec{\omega}) = g(\omega)U(\hat{\omega})$, where $U(\hat{\omega}) = (1/4\pi)$. With the above form of $G(\vec{\omega})$, we calculate that [41]

$$\mathbf{J}(s) = \left(\frac{1}{3s} + \frac{2s}{3}\int_0^{+\infty}\frac{g(\omega)}{s^2+\omega^2}d\omega\right)\mathbf{I} \triangleq h(s)\mathbf{I}. \quad (8)$$

The dispersion relation in Eq. (7) finally reduces to

$$1 - \frac{2K}{3}h(s) - \frac{K}{3}h(s+2a^2) = 0. \qquad (9)$$

For $K \to 0$, $s \to 0$, the behavior of s in Eq. (9) for K around zero is represented by $s = \frac{2}{9}K$ [41]. Thus, we can ascertain that the incoherent state will be stable for $K < 0$ and unstable for $K > 0$, which is valid independent of $g(\omega)$. For $D = 3$, we have proved that the incoherence loses its stability at $K_c = 0$, which is exactly the same as that of the 3D Kuramoto model [17], in turn confirming that our model [Eq. (1)] reduces to the D-dimensional Kuramoto model in the limit $K \to 0$.

ii) Stability of locking and amplitude death. Locked states correspond to fixed points of Eq. (1), for which $\vec{p}$ is a constant vector with $p > 0$. In contrast, amplitude death refers to the coupling-induced stabilization of $\vec{r}_i = \vec{0}$, for which $p = 0$. Theoretically, the stability of locked states and amplitude death can be analyzed at the same time. For $N \to \infty$, in the locked state, the position $\vec{r}_i$ of the ith oscillator is determined by its natural rotation $\mathbf{W}_i$. Therefore, $\vec{r}$ is regarded as a function of $\mathbf{W}$ instead of the subscript i, which obeys

$$\frac{d\vec{r}_F}{dt} = (1 - K - |\vec{r}_F|^2)\vec{r}_F + \mathbf{W}\vec{r}_F + K\vec{p}_F = 0, \qquad (10)$$

with the subscript F indicating that the oscillator is at a fixed point. The order parameter is then written

by $\vec{p}_F = \int_{\mathbb{R}^{D(D-1)/2}}\vec{r}_F G(\vec{\omega})d\vec{\omega}$, whose magnitude p_F satisfies [41]

$$Kp_F^2 = \int_{\mathbb{R}^{D(D-1)/2}}(|\vec{r}_F|^2 - 1 + K)|\vec{r}_F|^2 G(\vec{\omega})d\vec{\omega}, \quad (11)$$

which holds for all $D \geq 2$. For $D = 3$, $\mathbf{W}\vec{r}_F = \vec{\omega}\times\vec{r}_F$, and Eq. (10) can be solved to obtain [41]

$$\vec{r}_F = \frac{K}{(\mu^2+\omega^2)}(\mu\vec{p}_F + \nu\vec{\omega} + \vec{\omega}\times\vec{p}_F), \qquad (12)$$

with $\mu = |\vec{r}_F|^2 - 1 + K$ and $\nu = (\vec{p}_F\cdot\vec{\omega})/\mu$, where μ and ν obey $(\mu + 1 - K)(\mu^2+\omega^2) = K^2(p_F^2+\nu^2)$. From Eq. (12), $\vec{r}_F$ always exists for $D = 3$ once if $K > 0$, in contrast to $D = 2$, for which the locked state exists only for sufficiently large K [43–45].

To determine the stability of locked states in the infinite-N limit, one has to consider both the discrete and the continuous spectra of the linearized system of Eq. (10) around $\vec{r}_F$. For $D \geq 2$ and $N \to \infty$, we find the continuous and the discrete spectra given by [41]

$$\det(s\mathbf{I} - \mathbf{M}) = 0 \qquad (13)$$

and

$$\det\left(\mathbf{I} - K\int_{\mathbb{R}^{D(D-1)/2}}(s\mathbf{I}-\mathbf{M})^{-1}G(\vec{\omega})d\vec{\omega}\right) = 0, \quad (14)$$

where $\mathbf{M} = \mathbf{W} - 2\vec{r}_F\vec{r}_F^T + (1 - |\vec{r}_F|^2 - K)\mathbf{I}$. The locked solutions are stable if both Eqs. (13) and (14) have only roots s with $\text{Re}(s) < 0$.

By setting $\vec{r}_F = \vec{0}$, Eqs. (14) and (13) yield the discrete and the continuous spectra governing the stability of amplitude death for $N \to \infty$, which can also be obtained by performing a stability analysis of Eq. (1) around $\vec{r}_i = \vec{0}$ [41]. The continuous spectrum can be proved to be stable if $K > 1$ for all $D \geq 2$ [50], whereas its discrete spectrum cannot be worked out explicitly for a general $G(\vec{\omega})$. Here, we analytically solve the stability of amplitude death for all $D \geq 2$, in contrast to the earlier works (Refs. [45,46]) that were confined to $D = 2$.

For $D = 3$, by writing $G(\vec{\omega}) = g(\omega)U(\hat{\omega})$, the discrete spectrum for amplitude death further reduces to [41]

$$h(s - 1 + K) = \frac{1}{K}, \qquad (15)$$

with the function h defined as in Eq. (8). Amplitude death is stable if Eq. (15) has only roots with negative real parts for $K > 1$.

For example, for $D = 3$, if each element of $\vec{\omega}_i$ is picked randomly according to $\omega_{ji} \sim Norm(0, \Delta^2)$ for $j = 1, 2, 3$, the distribution of the natural rotations can be written as
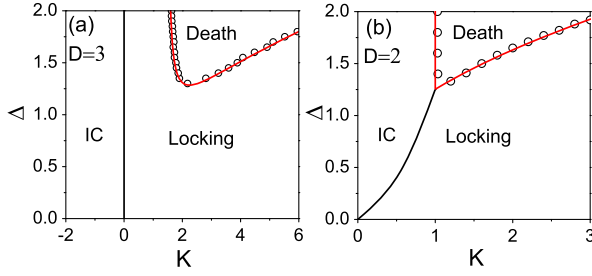
FIG. 2. Phase diagram for the system in Eq. (1) with $D(D-1)/2$ elements of $\mathbf{W}_i$ distributed according to $Norm(0, \Delta^2)$ for (a) $D = 3$ and (b) $D = 2$. The black and red curves denote the boundaries of incoherence (IC) and amplitude death determined theoretically, whereas the open circles are the simulation results of the amplitude death boundary by integrating Eq. (1) with $N = 5000$.

$G(\vec{\omega}) = g(w)U(\hat{\omega})$, where the distribution of the rotation directions is isotropic and the distribution of the magnitudes is described by $g(\omega) = \sqrt{(2/\pi)}(\omega^2/\Delta^3)e^{-\omega^2/(2\Delta^2)}$ [51]. By setting $s = 0$ in Eq. (15), we obtain the boundary of the stable amplitude death region governed by [41]

$$\frac{1}{3(K-1)} + \frac{2(K-1)}{3} \int_0^{+\infty} \frac{g(\omega)}{(K-1)^2 + \omega^2} d\omega = \frac{1}{K}, \quad (16)$$

which is represented by the red curve in Fig. 2(a) depicting the phase diagram of the system in the (K, Δ) parameter space for $D = 3$. Note that the theoretical prediction by Eq. (16) is rather accurate and well confirmed by the simulation results. For comparison, Fig. 2(b) depicts the phase diagram for $D = 2$ with $w_i \sim Norm(0, \Delta^2)$. For $D \geq 4$, the phase diagrams, qualitatively similar to Figs. 2(a) and 2(b) for odd and even dimensions, have been corroborated numerically.

For $K > 0$, aside from the coherent fixed-point solutions (locked states and amplitude death)—Eq. (1) may also have oscillatory time-dependent solutions—i.e., the system could display *rhythmic states* [20], characterized by an unsteady motion of p. For example, Figs. 3(a) and 3(b) show two numerical observations of a time-dependent evolution of p for Eq. (1) with $D = 3$, where $\vec{\omega}_i$ values are sampled according to $G(\vec{\omega}) = \delta(\omega - \omega_0)U(\hat{\omega})$. Figure 3(c) further depicts p vs K. Again, the incoherent state is observed only for $K < 0$, and becomes unstable for $K > 0$, which is in accordance with the theoretical prediction of the incoherence. Interestingly, as K is gradually increased from zero, rhythmic states appear and persist for a large interval of $K > 0$, where the periodic dynamics of p emerges through the similarly periodic oscillations in the magnitudes of $\vec{r}_i$'s. After the rhythmic state turning to unstable, the system transits to locked states and amplitude death. For $G(\vec{\omega}) = \delta(\omega - \omega_0)U(\hat{\omega})$ considered above [i.e., $g(\omega) = \delta(\omega - \omega_0)$], the stable coupling interval for amplitude death is derived as [41]
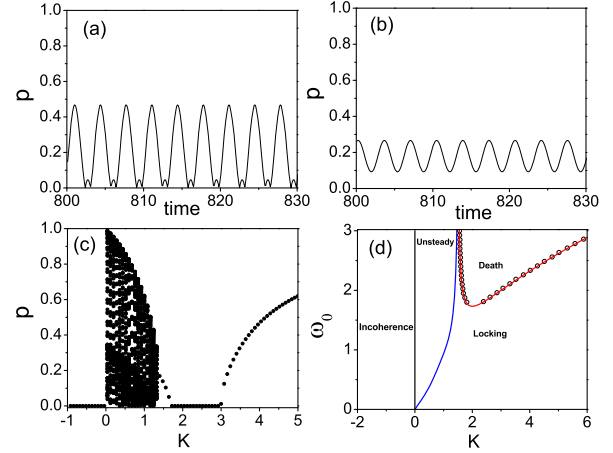

FIG. 3. Results for the system in Eq. (1) with $D = 3$, where $\vec{\omega}_i$ values are now sampled according to $G(\vec{\omega}) = \delta(\omega - \omega_0)U(\hat{\omega})$. (a) $p(t)$ for $K = 1.2$. (b) $p(t)$ for $K = 1.36$. (c) p vs K; $\omega_0 = 2$ is fixed. (d) Phase diagram in the parameter space of (K, ω_0). The red curve represents the theoretical prediction for the stable coupling interval of amplitude death given by Eq. (17), which is well confirmed by the numerical results marked by the open circles. The blue curve denotes the unsteady-locking boundary determined numerically.

$$\frac{\omega_0^2 + 3 - \omega_0\sqrt{\omega_0^2 - 3}}{3} < K < \frac{\omega_0^2 + 3 + \omega_0\sqrt{\omega_0^2 - 3}}{3} \quad (17)$$

for $\omega_0 > \sqrt{3}$. For $D = 3$, amplitude death is fundamentally induced by the orientational disorder for a large fixed rotation magnitude, which is distinctly different from the case of $D = 2$, where amplitude death arises owing to a sufficiently large spread of the natural frequencies [43–45]. In fact, amplitude death is impossible to be stabilized for the case of $D = 3$ in the absence of orientational disorder [41]. For a global view, Fig. 3(d) portrays the phase diagram of the system in the (K, ω_0) plane. Clearly, the system in Eq. (1) can experience both steady behaviors and rhythmic states if $\vec{\omega}_i$ is sampled according to $G(\vec{\omega}) = \delta(\omega - \omega_0)U(\hat{\omega})$ [52].

To conclude, we have introduced and studied a new model of globally coupled D-dimensional generalized limit-cycle oscillators with amplitude dynamics. Under the weak coupling limit $K \to 0$, our model reduces to the D-dimensional Kuramoto phase model, which is akin to a similar classic construction of the seminal Kuramoto phase model from weakly coupled two-dimensional limit-cycle oscillators [47,48]. In this sense, our work puts the recent studies regarding the D-dimensional Kuramoto model [17–25] on a stronger footing by providing a much more general framework to consider the previous results, owing to no longer being constrained by fixed amplitude dynamics. Thus, our model may find strong potential for actual applications in a wider range of physical, biological, and technological systems involving quenched random rotation axes and frequencies, such as leading to a deeper

understanding of the collective motion in three-dimensional swarming systems with helical trajectories [13], the spatiotemporal alignment of beating cilia [53], the ferromagnetic resonance in biomagnetism [54], etc. It should be highlighted that the emergence of rhythmic states in the model in Eq. (1) strongly depends on the distribution $G(\vec{\omega})$, whose underlying principles as well as the necessary or sufficient conditions on the distribution $G(\vec{\omega})$ that lead to rhythmic states for $D \geq 3$ deserve a detailed study, which would be the scope of future work. Further, there also lies the possibility of various extensions of our model, such as including the role of noise, external forces, network-based coupling, etc., which may open up a prosperously new area of research and will have great impacts in the field of nonlinear (collective) dynamics and complex systems.

---

[*]Corresponding author.
 weizou83@gmail.com

[1] Y. Kuramoto, *Chemical Oscillations, Waves, and Turbulence* (Springer, Berlin, 1984).

[2] A. Pikovsky, M. Rosenblum, and J. Kurths, *Synchronization: A Universal Concept in Nonlinear Sciences* (Cambridge University Press, Cambridge, England, 2003).

[3] S. H. Strogatz, *Sync: The Emerging Science of Spontaneous Order* (Hyperion, New York, 2003).

[4] S. Boccaletti, A. N. Pisarchik, C. I. del Genio, and A. Amann, *Synchronization: From Coupled Systems to Complex Networks* (Cambridge University Press, Cambridge, England, 2018).

[5] A. T. Winfree, *The Geometry of Biological Time* (Springer, New York, 1980).

[6] T. Vicsek, A. Czirók, E. Ben-Jacob, I. Cohen, and O. Shochet, Novel Type of Phase Transition in a System of Self-Driven Particles, Phys. Rev. Lett. **75**, 1226 (1995).

[7] G. Grégoire and H. Chaté, Onset of Collective and Cohesive Motion, Phys. Rev. Lett. **92**, 025702 (2004).

[8] Y. Kuramoto, Self-entrainment of a population of coupled non-linear oscillators, in *Proceedings of the International Symposium on Mathematical Problems in Theoretical Physics*, edited by H. Araki, Lecture notes in Physics, Vol. 39 (Springer, Berlin, 1975), pp. 420–422.

[9] S. H. Strogatz, From Kuramoto to Crawford: Exploring the onset of synchronization in populations of coupled oscillators, Physica (Amsterdam) **143D**, 1 (2000).

[10] J. A. Acebrón, L. L. Bonilla, C. J. Pérez Vicente, F. Ritort, and R. Spigler, The Kuramoto model: A simple paradigm for synchronization phenomena, Rev. Mod. Phys. **77**, 137 (2005).

[11] I. Z. Kiss, Y. Zhai, and J. L. Hudson, Emerging coherence in a population of chemical oscillators, Science **296**, 1676 (2002).

[12] F. Ritort, Solvable Dynamics in a System of Interacting Random Tops, Phys. Rev. Lett. **80**, 6 (1998).

[13] C. M. Zheng, R. Toenjes, and A. Pikovsky, Transition to synchrony in a three-dimensional swarming model with helical trajectories, Phys. Rev. E **104**, 014216 (2021).

[14] R. Olfati-Saber, Swarms on sphere: A programmable swarm with synchronous behaviors like oscillator networks, in *Proceedings of the 45th IEEE Conference on Decision and Control* (IEEE, New York, 2006), pp. 5060–5066.

[15] J. Zhu, Synchronization of Kuramoto model in a high-dimensional linear space, Phys. Lett. A **377**, 2939 (2013).

[16] T. Tanaka, Solvable model of the collective motion of heterogeneous particles interacting on a sphere, New J. Phys. **16**, 023016 (2014).

[17] S. Chandra, M. Girvan, and E. Ott, Continuous Versus Discontinuous Transitions in the *D*-Dimensional Generalized Kuramoto Model: Odd *D* is Different, Phys. Rev. X **9**, 011002 (2019).

[18] S. Chandra, M. Girvan, and E. Ott, Complexity reduction ansatz for systems of interacting orientable agents: Beyond the Kuramoto model, Chaos **29**, 053107 (2019).

[19] S. Chandra and E. Ott, Observing microscopic transitions from macroscopic bursts: Instability-mediated resetting in the incoherent regime of the *D*-dimensional generalized Kuramoto model, Chaos **29**, 033124 (2019).

[20] X. Dai, X. Li, H. Guo, D. Jia, M. Perc, P. Manshour, Z. Wang, and S. Boccaletti, Discontinuous Transitions and Rhythmic States in the *D*-Dimensional Kuramoto Model Induced by a Positive Feedback with the Global Order Parameter, Phys. Rev. Lett. **125**, 194101 (2020).

[21] K. Kovalenko, X. Dai, K. Alfaro-Bittner, A. M. Raigorodskii, M. Perc, and S. Boccaletti, Contrarians Synchronize Beyond the Limit of Pairwise Interactions, Phys. Rev. Lett. **127**, 258301 (2021).

[22] X. Dai, K. Kovalenko, M. Molodyk, Z. Wang, X. Li, D. Musatov, A. M. Raigorodskii, K. Alfaro-Bittner, G. D. Cooper, G. Bianconi, and S. Boccaletti, *D*-dimensional oscillators in simplicial structures: Odd and even dimensions display different synchronization scenarios, Chaos Soliton Fract. **146**, 110888 (2021).

[23] M. Lipton, R. Mirollo, and S. H. Strogatz, The Kuramoto model on a sphere: Explaining its low-dimensional dynamics with group theory and hyperbolic geometry, Chaos **31**, 093113 (2021).

[24] A. E. D. Barioni and M. A. M. de Aguiar, Complexity reduction in the 3*D* Kuramoto model, Chaos Soliton Fract. **149**, 111090 (2021).

[25] A. E. D. Barioni and M. A. M. de Aguiar, Ott-Antonsen ansatz for the *D*-dimensional Kuramoto model: A constructive approach, Chaos **31**, 113141 (2021).

[26] Y. Katz, K. Tunstrøm, C. C. Ioannou, C. Huepe, and I. D. Couzin, Inferring the structure and dynamics of interactions in schooling fish, Proc. Natl. Acad. Sci. U.S.A. **108**, 18720 (2011).

[27] T. Vicsek and A. Zafeiris, Collective motion, Phys. Rep. **517**, 71 (2012).

[28] K. P. O'Keeffe, H. Hong, and S. H. Strogatz, Oscillators that sync and swarm, Nat. Commun. **8**, 1504 (2017).

[29] D. J. Sumpter, *Collective Animal Behavior* (Princeton University Press, Princeton, NJ, 2010).

[30] E. D. Fagerholm, R. J. Moran, I. R. Violante, R. Leech, and K. J. Friston, Dynamic causal modelling of phase-amplitude interactions, NeuroImage **208**, 116452 (2020).

[31] D. Wilson and B. Ermentrout, Phase Models Beyond Weak Coupling, Phys. Rev. Lett. **123**, 164101 (2019).

[32] B. Heinrich, Y. Tserkovnyak, G. Woltersdorf, A. Brataas, R. Urban, and G. E. W. Bauer, Dynamic Exchange Coupling in Magnetic Bilayers, Phys. Rev. Lett. **90**, 187601 (2003).

[33] S. Klingler, V. Amin, S. Geprägs, K. Ganzhorn, H. Maier-Flaig, M. Althammer, H. Huebl, R. Gross, R. D. McMichael, M. D. Stiles, S. T. B. Goennenwein, and M. Weiler, Spin-Torque Excitation of Perpendicular Standing Spin Waves in Coupled YIG/Co Heterostructures, Phys. Rev. Lett. **120**, 127201 (2018).

[34] J. T. Young, A. V. Gorshkov, M. Foss-Feig, and M. F. Maghrebi, Nonequilibrium Fixed Points of Coupled Ising Models, Phys. Rev. X **10**, 011039 (2020).

[35] J. Yan, M. Bloom, S. C. Bae, E. Luijten, and S. Granick, Linking synchronization to self-assembly using magnetic Janus colloids, Nature (London) **491**, 578 (2012).

[36] A. Snezhko and I. S. Aranson, Magnetic manipulation of self-assembled colloidal asters, Nat. Mater. **10**, 698 (2011).

[37] J. E. Martin and A. Snezhko, Driving self-assembly and emergent dynamics in colloidal suspensions by time-dependent magnetic fields, Rep. Prog. Phys. **76**, 126601 (2013).

[38] N. H. Nguyen, D. Klotsa, M. Engel, and S. C. Glotzer, Emergent Collective Phenomena in a Mixture of Hard Shapes Through Active Rotation, Phys. Rev. Lett. **112**, 075701 (2014).

[39] B. C. van Zuiden, J. Paulose, W. T. Irvine, D. Bartolo, and V. Vitelli, Spatiotemporal order and emergent edge currents in active spinner materials, Proc. Natl. Acad. Sci. U.S.A. **113**, 12919 (2016).

[40] For $D = 2$, $\mathbf{W}_i = \begin{pmatrix} 0 & -\omega_i \\ \omega_i & 0 \end{pmatrix}$ is characterized only by one scalar parameter ω_i, which denotes the natural frequency of the ith uncoupled oscillator. For $D = 3$, $\mathbf{W}_i = \begin{pmatrix} 0 & -\omega_{3i} & \omega_{2i} \\ \omega_{3i} & 0 & -\omega_{1i} \\ -\omega_{2i} & \omega_{1i} & 0 \end{pmatrix}$, $\mathbf{W}_i \vec{r}_i = \vec{\omega}_i \times \vec{r}_i$, where $\vec{\omega}_i = (\omega_{1i}, \omega_{2i}, \omega_{3i})^T$ denotes the particle velocity (frequency) vector [13] or the natural rotation of the ith oscillator [17], as each uncoupled element $\vec{r}_i$ precesses around the vector $\hat{\omega}_i = \vec{\omega}_i/|\vec{\omega}_i|$ at the rotation rate $\omega_i = |\vec{\omega}_i|$ on the surface of the unit sphere [41]. Note that, for $D \geq 4$, the vector $\vec{\omega}_i$ associated with $\mathbf{W}_i$ has $D(D-1)/2$ independent parameters, whose dimension is higher than that of the D-dimensional state variable $\vec{r}_i$. For example, for $D = 4$, $\mathbf{W}_i = \begin{pmatrix} 0 & -\omega_{6i} & \omega_{5i} & -\omega_{4i} \\ \omega_{6i} & 0 & -\omega_{3i} & \omega_{2i} \\ -\omega_{5i} & \omega_{3i} & 0 & -\omega_{1i} \\ \omega_{4i} & -\omega_{2i} & \omega_{1i} & 0 \end{pmatrix}$ is completely determined by the six-dimensional vector $\vec{\omega}_i = (\omega_{1i}, \omega_{2i}, \omega_{3i}, \omega_{4i}, \omega_{5i}, \omega_{6i})^T$. Via a relatively common interpretation of rotation in higher dimensions through the special orthogonal group generated by skew-symmetric matrices, $\vec{\omega}_i$ (i.e., $\mathbf{W}_i$) can also be reasonably interpreted as the natural rotation of the ith uncoupled oscillator of higher dimensions with $D \geq 4$. It should be highlighted that the case of $D = 3$ is of practical interest, and that the complexity grows significantly with the increase of the dimension D for both the theoretical analyses and the numerical simulations of the model.

[41] See Supplemental Material at http://link.aps.org/supplemental/10.1103/PhysRevLett.130.107202 for the details on the dynamics of the model for $D = 3$ and $K = 0$, the reduction of the model in the weak coupling limit $K \to 0$, the derivations of Eqs. (7), (11)–(17), the calculation of Eq. (8), the analysis of Eq. (9), the validation of the distribution $G(\vec{\omega}) = g(w)U(\hat{\omega})$ for $D = 3$, the linear stability analysis of amplitude death for $N < \infty$, and the proof of the instability of amplitude death in the absence of orientational disorder for $D = 3$.

[42] M. Shiino and M. Frankowicz, Synchronization of infinitely many coupled limit-cycle type oscillators, Phys. Lett. A **136**, 103 (1989).

[43] P. C. Matthews and S. H. Strogatz, Phase Diagram for the Collective Behavior of Limit-Cycle Oscillators, Phys. Rev. Lett. **65**, 1701 (1990).

[44] P. C. Matthews, R. E. Mirollo, and S. H. Strogatz, Dynamics of a large system of coupled nonlinear oscillators, Physica (Amsterdam) **52D**, 293 (1991).

[45] R. E. Mirollo and S. H. Strogatz, Amplitude death in an array of limit-cycle oscillators, J. Stat. Phys. **60**, 245 (1990).

[46] G. B. Ermentrout, Oscillator death in populations of "all to all" coupled nonlinear, Physica (Amsterdam) **41D**, 219 (1990).

[47] I. León and D. Pazó, Phase reduction beyond the first order: The case of the mean-field complex Ginzburg-Landau equation, Phys. Rev. E **100**, 012211 (2019).

[48] I. León and D. Pazó, Enlarged Kuramoto model: Secondary instability and transition to collective chaos, Phys. Rev. E **105**, L042201 (2022).

[49] The *ansatz* for the small perturbation is of the form $F = F_0 + \varepsilon e^{st} \xi(r, \theta, \phi, \vec{\omega})$ ($0 < \varepsilon \ll 1$), where s is the characteristic exponent used to characterize the growth rate of the perturbation. If all the real parts of s are negative, the perturbation decays exponentially in time, thus the incoherent state is stable. In contrast, if s has a positive real part, the incoherent state becomes unstable, because the perturbation grows exponentially.

[50] The continuous spectrum for amplitude death is given by roots of $\det((s - 1 + K)\mathbf{I} - \mathbf{W}) = 0$, where $\mathbf{W}$ is an antisymmetric matrix. By applying the fact that the real part of all the eigenvalues of any real antisymmetric matrix is zero, it can be directly deduced that the continuous spectrum for amplitude death is stable for $K > 1$.

[51] The amplitudes (magnitudes) of 3D vectors with Gaussian random components are distributed according to the Maxwell-Boltzmann distribution, which is the classical result that deserves an honorable mention. The detailed derivations for the distribution of the magnitudes $g(\omega)$ for the case of $D = 3$ are provided in the Supplemental Material.

[52] If each element of $\vec{\omega}_i$ is independently picked randomly according to $Norm(0, \Delta^2)$, only steady behaviors (i.e., incoherence, locking, and amplitude death) have been

found in our numerical simulations. However, for $G(\vec{\omega}) = \delta(\omega - \omega_0)U(\hat{\omega})$, rhythmic states have been reliably uncovered numerically in the model for $D = 3$. In fact, a rhythmic (periodic) state has also been numerically found for the 3D Kuramoto phase model with the same distribution $G(\vec{\omega}) = \delta(\omega - \omega_0)U(\hat{\omega})$ in Ref. [24]. In our simulations, we have only observed the periodic oscillations of p. However, it does not rule out the possibility of quasiperiodic or chaotic evolution of p for other distributions $G(\vec{\omega})$. For the model in Eq. (1) with $D = 2$, both quasiperiodic and chaotic behaviors of p have been numerically observed for the uniform frequency distribution [43,44], whereas only steady behaviors have been reported

for the Lorentzian frequency distribution [42]. By adopting a special distribution similar to $G(\vec{\omega}) = \delta(\omega - \omega_0)U(\hat{\omega})$ used for $D = 3$, we have numerically observed the rhythmic states and other aspects of the bifurcation and phase diagrams (i.e., incoherence, amplitude death, and locking) as shown in Fig. 3 for the case of $D = 4$, which may also appear in other higher odd and even dimensions with $D > 4$ for particular choices of $G(\vec{\omega})$.

[53] T. Niedermayer, B. Eckhardt, and P. Lenz, Synchronization, phase locking, and metachronal wave formation in ciliary chains, Chaos **18**, 037128 (2008).

[54] S. V. Vonsovskii, *Ferromagnetic Resonance* (Pergamon Press, New York, 1966).